

This article was downloaded by:

On: 23 January 2011

Access details: *Access Details: Free Access*

Publisher *Taylor & Francis*

Informa Ltd Registered in England and Wales Registered Number: 1072954 Registered office: Mortimer House, 37-41 Mortimer Street, London W1T 3JH, UK



Journal of Coordination Chemistry

Publication details, including instructions for authors and subscription information:

<http://www.informaworld.com/smpp/title~content=t713455674>

Syntheses, crystal structures, and magnetic properties of RE(III)-Cu(II) heteronuclear complexes with α -methylacrylic acid

Fang Chen^a; Weimin Lu^a; Yue Zhu^b; Bin Wu^c; Xiaoming Zheng^a

^a Department of Chemistry, Zhejiang University (Xixi Campus), Hangzhou, 310028, P.R. China ^b

Department of Basic Medical Sciences, Hangzhou Normal University, Hangzhou, 310018, P.R. China ^c

Department of Chemistry, Zhejiang Sci-Tech University, Hangzhou, 310018, P.R. China

First published on: 08 September 2010

To cite this Article Chen, Fang , Lu, Weimin , Zhu, Yue , Wu, Bin and Zheng, Xiaoming(2010) 'Syntheses, crystal structures, and magnetic properties of RE(III)-Cu(II) heteronuclear complexes with α -methylacrylic acid', Journal of Coordination Chemistry, 63: 20, 3599 – 3609, First published on: 08 September 2010 (iFirst)

To link to this Article: DOI: 10.1080/00958972.2010.514904

URL: <http://dx.doi.org/10.1080/00958972.2010.514904>

PLEASE SCROLL DOWN FOR ARTICLE

Full terms and conditions of use: <http://www.informaworld.com/terms-and-conditions-of-access.pdf>

This article may be used for research, teaching and private study purposes. Any substantial or systematic reproduction, re-distribution, re-selling, loan or sub-licensing, systematic supply or distribution in any form to anyone is expressly forbidden.

The publisher does not give any warranty express or implied or make any representation that the contents will be complete or accurate or up to date. The accuracy of any instructions, formulae and drug doses should be independently verified with primary sources. The publisher shall not be liable for any loss, actions, claims, proceedings, demand or costs or damages whatsoever or howsoever caused arising directly or indirectly in connection with or arising out of the use of this material.

Syntheses, crystal structures, and magnetic properties of RE(III)–Cu(II) heteronuclear complexes with α -methylacrylic acid

FANG CHEN[†], WEIMIN LU^{*†}, YUE ZHU[‡], BIN WU[§]
and XIAOMING ZHENG[†]

[†]Department of Chemistry, Zhejiang University (Xixi Campus), Hangzhou, 310028, P.R. China

[‡]Department of Basic Medical Sciences, Hangzhou Normal University, Hangzhou, 310018, P.R. China

[§]Department of Chemistry, Zhejiang Sci-Tech University, Hangzhou, 310018, P.R. China

(Received 17 December 2009; in final form 2 July 2010)

A series of carboxylate-bridged heteronuclear 3d–4f complexes have been prepared by reaction of REL_3 ($HL = CH_2 = C(CH_3)COOH$) with $Cu(NO_3)_2$. A family of air-stable 2-D complexes $[RECuL_4(H_2O)_4]_n L_n$ ($RE = La$ (**1**), Ce (**2**), Eu (**3**), and Gd (**4**)) have the same crystal system (monoclinic) and space group ($P2_1/c$). The chains which are made by the carboxylate-bridged alternating $Cu(II)$ – $RE(III)$ fragments spreading along the c -axis are linked through hydrogen bonds by uncoordinated carboxylates to form a 2-D network structure along the bc planes. Magnetic measurements showed that **1** and **2** have antiferromagnetic interaction between RE and Cu , but **4** exhibits ferromagnetic interaction. Eu ions show van Vleck behavior in **3**.

Keywords: Rare earth; Copper; α -Methylacrylic acid; Crystal structure; Magnetic property

1. Introduction

A number of 3d and 4f heterometallic complexes have been studied for both their magnetic and chemical interests [1–4]. The relationship between magnetic interaction and structure of rare-earth ions coordinated with the first-series transition metals was explored to understand the magnetic exchange mechanism, which offered reliable theory to use crystal engineering for designing and synthesizing new molecule-based magnets of RE –transition-metal heteronuclear complexes and to improve the properties of RE functional materials.

Complexes with different dimensional frameworks have also attracted much attention for magnetic interaction, especially coupling between $Cu(II)$ and $Gd(III)$ [5–7]. Although a few exceptions are observed [8–10], recent studies have further revealed that the magnitude of ferromagnetic exchange interaction between different

*Corresponding author. Email: weimlu2000@163.com

metal centers is exponentially dependent on the Cu–Gd distance [11, 12] and the dihedral angle α defined by the two OCuO and OGDd planes of the bridging network [13]. In the course of our investigations into 3d–4f complexes, we have reported a series of zero dimension M(II)–RE(III) complexes with carboxylate bridges and neutral ligands (2,2'-bipyridine, 4,4'-bipyridine, 1,10-phenanthroline) over the past decade [14–20]. In this article, a series of isostructural complexes comprised of RE(III) (RE = La, Ce, Eu, Gd) and Cu(II) without neutral ligands have been synthesized and characterized, extending the number of known examples and understanding of magnetic interaction of Gd(III)–Cu(II). Following the approach proposed by Kahn *et al.* [7], we examine the magnetic interaction between Gd(III) and Cu(II).

2. Experimental

2.1. Materials and measurements

REL₃ were synthesized according to the literature [21]. All chemicals used in this work were commercially obtained without purification. Elemental analyses for C and H were performed on an Eager 200 instrument. The IR spectrum was recorded on a Nicolet 560 spectrophotometer from 4000 to 400 cm⁻¹ using a powdered sample spread on a KBr plate. Variable temperature susceptibilities were measured by physical property measurement system PPMS-9 from 5 to 300 K at a magnetic field of 20 kOe for **1** or 10 kOe for **2** and **3**. Variable temperature susceptibilities of **4** were measured by magnetic property measurement system MPMS(SQUID)-XL-5 from 4.2 to 300 K at a magnetic field of 10 kOe. The molar susceptibilities were corrected from the sample holder and diamagnetic contributions of all constituent atoms by using Pascal's constants.

2.2. Synthesis of [RECu(L₄(H₂O)₄)_nL_n (RE = La, Ce, Eu, Gd)]

REL₃ (0.80 mmol) was dissolved in 5 mL H₂O and 1 mL ethanol and the pH adjusted to 4.1 with HL (1 mol L⁻¹). A solution of Cu(NO₃)₂ (2.4 mL, 1 mol L⁻¹) was added with stirring. After filtration, the filtrate was allowed to stand at room temperature and blue single crystals suitable for X-ray diffraction were obtained after several weeks. Anal. Calcd for **1**, [LaCuL₄(H₂O)₄]L (%) : C, 34.32; H, 4.75. Found (%): C, 34.16; H, 4.72. IR (KBr): $\nu_{\text{as(COO)}}$ 1539 cm⁻¹, $\nu_{\text{s(COO)}}$ 1423 cm⁻¹, $\nu_{\text{(C=C)}}$ 1645 cm⁻¹. Anal. Calcd for **2**, [CeCuL₄(H₂O)₄]L (%) : C, 34.26; H, 4.74. Found (%): C, 34.52; H, 4.68. IR (KBr): $\nu_{\text{as(COO)}}$ 1537 cm⁻¹, $\nu_{\text{s(COO)}}$ 1423 cm⁻¹, $\nu_{\text{(C=C)}}$ 1647 cm⁻¹. Anal. Calcd for **3**, [EuCuL₄(H₂O)₄]L (%) : C, 33.69; H, 4.67. Found (%): C, 33.78; H, 4.80. IR (KBr): $\nu_{\text{as(COO)}}$ 1541 cm⁻¹, $\nu_{\text{s(COO)}}$ 1423 cm⁻¹, $\nu_{\text{(C=C)}}$ 1645 cm⁻¹. Anal. Calcd for **4**, [GdCuL₄(H₂O)₄]L (%) : C, 33.44; H, 4.63. Found (%): C, 33.40; H, 4.58. IR (KBr): $\nu_{\text{as(COO)}}$ 1537 cm⁻¹, $\nu_{\text{s(COO)}}$ 1417 cm⁻¹, $\nu_{\text{(C=C)}}$ 1643 cm⁻¹. The $\nu_{\text{as(COO)}}$ and $\nu_{\text{s(COO)}}$ of the complexes are different from those (1612 and 1551 cm⁻¹) of polymer [LaCu(PDC)₂H₂O]_n [22].

2.3. Crystal structure determination for the complexes

Each crystal was mounted on a glass fiber. Unit cell and intensity data were measured on a Rigaku RIGAKU-RAPID diffractometer with graphite-monochromated Mo- $K\alpha$ radiation ($\lambda = 0.71073 \text{ \AA}$) by the $\omega = 2\theta$ scan technique at room temperature. Usual Lp and empirical absorption corrections were applied. The structures were solved by direct methods and then by Fourier syntheses expanded using the Fourier technique. The structure refinement was carried out by full-matrix least-squares on F^2 with anisotropic thermal parameters for all non-hydrogen atoms using the SHELXTL/PC program package [23]. Hydrogens were geometrically fixed and allowed to ride on the parent carbons with isotropic displacement parameters. Atomic scattering factors were taken from International Tables for X-ray Crystallography [24]. Crystallographic data and structural refinements for **1–4** are summarized in table 1. Important bond lengths and angles are listed in table 2. More details on the crystallographic studies as well as atom displacement parameters are given in the “Supplementary material”.

3. Results and discussion

3.1. Crystal structure for the complexes

The crystal structure of $[\text{GdCuL}_4(\text{H}_2\text{O})_4]_n\text{L}_n$ consists of polycationic chains and acrylate anions. The polycationic chains are made by carboxylate-bridged alternating Cu(II)–Gd(III) fragments spreading along the c -axis.

As shown in figure 1, each Gd(III) is eight-coordinate by four oxygens of four waters ($\text{Gd–O} = 2.457\text{–}2.508 \text{ \AA}$) and four oxygens from four carboxylates ($\text{Gd–O} = 2.339\text{–}2.342 \text{ \AA}$). The configuration around Gd is a square antiprism, in which each square face consists of two aqua oxygens and two carboxylate oxygens from carboxylate bridges. The dihedral angle between two square faces [O(1), O(3), O(12), O(14)] and [O(11), O(13), O(5), O(7)] is close to 0° . The distances from Gd(II) to the planes are nearly the same (1.332 and 1.331 \AA , respectively). Each Cu(II) is four-coordinate by four oxygens from four carboxylates to form a distorted square plane [$\text{Cu–O} = 1.935\text{–}1.970 \text{ \AA}$]. The Cu(II) is almost situated at the center of the plane with the distance of 0.006 \AA between Cu(II) and the plane.

Two carboxylates use bidentate coordination to link Gd(III) and Cu(II). The intra-chain intermetallic distances of Gd–Cu and Gd^{iii} (symmetry code: $x, 1/2 - y, -1/2 + z$)–Cu are equal at 3.831 \AA , longer than those of Gd–Cu bridged by four carboxylates in $[\text{Cu}_2\text{Gd}_2(\text{bet})_{12}(\text{ClO}_4)_2](\text{ClO}_4)_8$ (3.595 \AA) [25] and in $[\text{CuGd}(\text{tza})_4(\text{H}_2\text{O})_5\text{Cl}]$ (3.777 \AA) [26], but shorter than that of Gd–Cu bridged by one carboxylate in $\{[\text{Cu}_3\text{Gd}_2(\text{oda})_6(\text{H}_2\text{O})_6]\cdot 12\text{H}_2\text{O}\}_n$ (4.662 \AA) [27]. The distance between Gd(III) and Cu(II) depends on the number of coordinated carboxylates. The angles Gd–Cu–Gd and Cu–Gd–Cu are 179.32° and 178.66° , respectively, so the chain runs in a nearly perfect line.

The polycationic chains are linked through hydrogen bonding (figure 2 and table 3) of uncoordinated carboxylates to form a 2-D network structure along the bc planes. Hydrogen bonding is often a primary interaction to form multidimensional

Table 1. Crystal data and structure refinement for the complexes.

Complexes	1	2	3	4
Empirical formula	$C_{20}H_{13}CuLaO_{14}$	$C_{20}H_{13}CeCuO_{14}$	$C_{20}H_{13}CuEuO_{14}$	$C_{20}H_{13}CuGdO_{14}$
Formula weight	699.91	701.12	712.96	718.25
Crystal system	Monoclinic	Monoclinic	Monoclinic	Monoclinic
Space group	$P2_1/c$	$P2_1/c$	$P2_1/c$	$P2_1/c$
Unit cell dimensions (\AA , $^\circ$)				
<i>a</i>	10.8069(9)	10.7704(2)	10.8535(6)	10.8502(6)
<i>b</i>	17.6348(11)	17.6001(5)	17.5333(12)	17.5313(11)
<i>c</i>	15.6276(11)	15.5354(1)	15.3264(9)	15.3228(9)
β	101.337(3)	101.325(1)	101.115(2)	101.162(2)
Volume (\AA^3), <i>Z</i>	2920.2(4), 4	2887.6(2), 4	2861.9(3), 4	2859.5(3), 4
<i>F</i> (000)	1404	1408	1428	1432
Calculated density (Mgm^{-3})	1.592	1.613	1.655	1.668
Absorption coefficient (mm^{-1})	2.231	2.353	2.975	3.103
Final <i>R</i> indices [<i>I</i> > 2 σ (<i>I</i>)]	$R_1 = 0.0525$, $wR_2 = 0.1254$	$R_1 = 0.0350$, $wR_2 = 0.0707$	$R_1 = 0.0639$, $wR_2 = 0.2096$	$R_1 = 0.0620$, $wR_2 = 0.1883$
<i>R</i> indices (all data)	$R_1 = 0.0973$, $wR_2 = 0.1535$	$R_1 = 0.0540$, $wR_2 = 0.0783$	$R_1 = 0.0856$, $wR_2 = 0.2267$	$R_1 = 0.0758$, $wR_2 = 0.1984$
Goodness-of-fit on <i>F</i> ²	0.991	1.136	1.103	1.061

Table 2. Selected bond distances (Å) and angles (°) for **1–4**.

	1	2	3	4
RE–O(1)	2.443(5)	2.416(3)	2.337(7)	2.339(8)
RE–O(3)	2.439(5)	2.415(3)	2.342(8)	2.339(7)
RE–O(5)	2.447(4)	2.418(2)	2.343(7)	2.342(7)
RE–O(7)	2.442(4)	2.419(3)	2.346(7)	2.341(7)
RE–O(11)	2.607(5)	2.551(3)	2.482(7)	2.508(8)
RE–O(12)	2.548(4)	2.537(3)	2.466(7)	2.457(8)
RE–O(13)	2.595(5)	2.577(3)	2.506(7)	2.485(8)
RE–O(14)	2.565(4)	2.517(3)	2.452(7)	2.469(8)
Cu–O(2)	1.976(5)	1.974(3)	1.964(8)	1.970(9)
Cu–O(4)	1.978(5)	1.973(2)	1.967(8)	1.965(9)
Cu–O(6)	1.962(4)	1.945(3)	1.932(7)	1.940(8)
Cu–O(8)	1.945(4)	1.950(3)	1.943(7)	1.935(8)
O(1)–RE–O(3)	85.85(17)	86.03(9)	87.1(3)	87.0(3)
O(1)–RE–O(5)	149.68(16)	147.85(10)	146.9(3)	148.6(3)
O(1)–RE–O(7)	102.43(16)	102.42(9)	101.7(3)	101.0(3)
O(1)–RE–O(11)	78.69(16)	78.51(90)	77.4(3)	77.7(3)
O(1)–RE–O(12)	76.96(16)	75.63(9)	75.5(3)	77.1(3)
O(1)–RE–O(13)	140.44(15)	141.29(9)	142.5(3)	141.1(3)
O(1)–RE–O(14)	68.72(15)	70.53(9)	71.1(3)	69.3(3)
O(3)–RE–O(5)	102.17(16)	102.13(10)	100.7(3)	101.6(3)
O(3)–RE–O(7)	148.09(16)	149.26(10)	148.5(3)	147.1(3)
O(3)–RE–O(11)	140.98(15)	140.47(9)	141.2(2)	142.3(3)
O(3)–RE–O(12)	70.19(15)	68.97(9)	69.1(3)	71.1(3)
O(3)–RE–O(13)	78.45(16)	78.78(9)	77.7(3)	77.4(3)
O(3)–RE–O(14)	76.18(15)	77.04(10)	77.2(3)	75.6(3)
O(5)–RE–O(7)	86.21(15)	86.42(9)	88.4(3)	88.2(3)
O(5)–RE–O(11)	76.89(17)	75.59(10)	76.7(3)	77.2(3)
O(5)–RE–O(12)	78.44(14)	78.47(9)	77.4(3)	77.3(3)
O(5)–RE–O(13)	69.74(15)	70.71(9)	70.3(3)	70.2(3)
O(5)–RE–O(14)	141.50(16)	141.49(9)	141.9(3)	142.1(3)
O(7)–RE–O(11)	70.780(15)	70.18(9)	70.1(3)	70.4(3)
O(7)–RE–O(12)	141.57(15)	141.67(9)	142.3(3)	141.7(3)
O(7)–RE–O(13)	75.75(16)	76.35(10)	77.2(3)	76.6(3)
O(7)–RE–O(14)	78.33(14)	78.12(9)	77.2(2)	77.5(3)
O(11)–RE–O(12)	71.49(15)	72.00(9)	72.6(3)	72.0(3)
O(11)–RE–O(13)	133.69(14)	133.35(8)	133.6(2)	133.8(2)
O(11)–RE–O(14)	128.38(16)	129.07(10)	128.2(3)	127.8(3)
O(12)–RE–O(13)	128.80(16)	128.91(10)	127.8(3)	128.3(3)
O(12)–RE–O(14)	133.05(14)	133.06(8)	133.2(2)	133.4(2)
O(13)–RE–O(14)	72.32(15)	71.43(9)	72.1(2)	72.4(3)
O(2)–Cu–O(4)	176.20(18)	177.12(10)	178.0(3)	178.3(3)
O(2)–Cu–O(6)	91.2(2)	90.36(12)	90.7(3)	90.8(4)
O(2)–Cu–O(8)	90.4(2)	88.30(12)	88.7(4)	90.0(4)
O(4)–Cu–O(6)	88.1(2)	90.40(12)	89.9(3)	88.8(4)
O(4)–Cu–O(8)	90.5(2)	91.06(12)	90.7(4)	90.3(4)
O(6)–Cu–O(8)	176.79(19)	177.09(11)	179.0(3)	178.7(3)

network structures, like in [Tb(pydc)(ox)_{1/2}(H₂O)₂] [28]. The intra- and inter-molecular hydrogen bonds decrease the energy and increase the stability of the structure. The inter-plane space is thus filled by carboxylates. The shortest inter-chain distance is 8.403 Å.

X-ray crystallography has revealed that **1**, **2**, and **3** are isomorphous to **4** with the analogous Cu–RE core. Only small metric differences are observed among them from the lanthanide contraction from La to Gd.

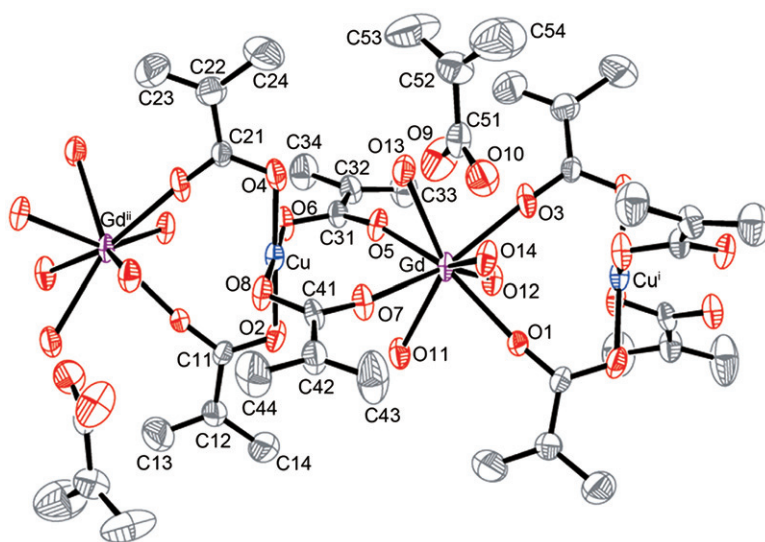


Figure 1. The molecular structure and atom-numbering scheme for $[\text{GdCu}_4(\text{H}_2\text{O})_4]\text{L}$. Displacement ellipsoids are shown at the 40% probability level and hydrogens have been omitted for clarity (symmetry code: ⁱ $x, 1/2 - y, 1/2 + z$; ⁱⁱ $x, 1/2 - y, -1/2 + z$).

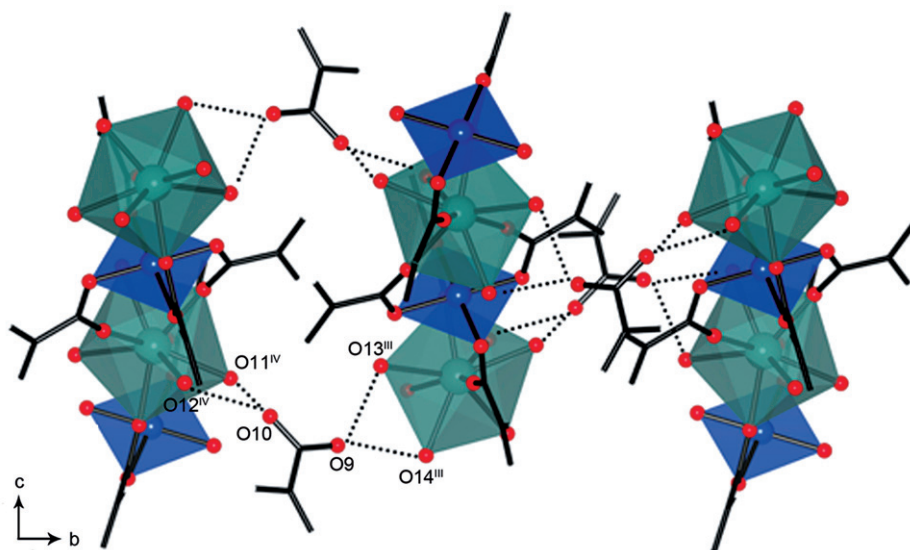


Figure 2. View of the structure of **4** down the a -axis. Hydrogen bonds are represented by dashed lines (symmetry codes: ⁱⁱⁱ $x, 1 + y, z$; ^{iv} $2 - x, 1/2 + y, 1/2 - z$).

3.2. Magnetic measurements for the complexes

Magnetic properties of the complexes are quite different although they are isomorphous crystals. The plots of $\chi_{\text{M}}T$ versus T for **1–3** are recorded in figure 3, where χ_{M} is molar magnetic susceptibility and T is temperature. The plot of **1** is almost flat down to 10 K

Table 3. Hydrogen bonding geometry for **4**.

	D–H	H...A	D...A	D–H...A
O(11)–H(111)...O(2) ⁽ⁱ⁾	0.92	1.94	2.848(11)	168
O(11)–H(112)...O(10) ^(v)	0.98	1.75	2.730(14)	176
O(12)–H(121)...O(8) ⁽ⁱⁱ⁾	0.98	1.90	2.878(11)	177
O(12)–H(122)...O(10) ^(v)	0.97	1.70	2.642(11)	165
O(13)–H(133)...O(4) ⁽ⁱ⁾	0.92	1.93	2.841(11)	172
O(13)–H(134)...O(9)	0.99	1.74	2.686(12)	159
O(14)–H(144)...O(9)	0.95	1.70	2.632(12)	165
O(14)–H(145)...O(6) ⁽ⁱⁱ⁾	0.95	1.96	2.885(11)	165

Symmetry code: ⁽ⁱ⁾ $x, 1/2 - y, 1/2 + z$; ⁽ⁱⁱ⁾ $x, 1/2 - y, -1/2 + z$; ^(v) $1 - x, -1/2 + y, 1/2 - z$.

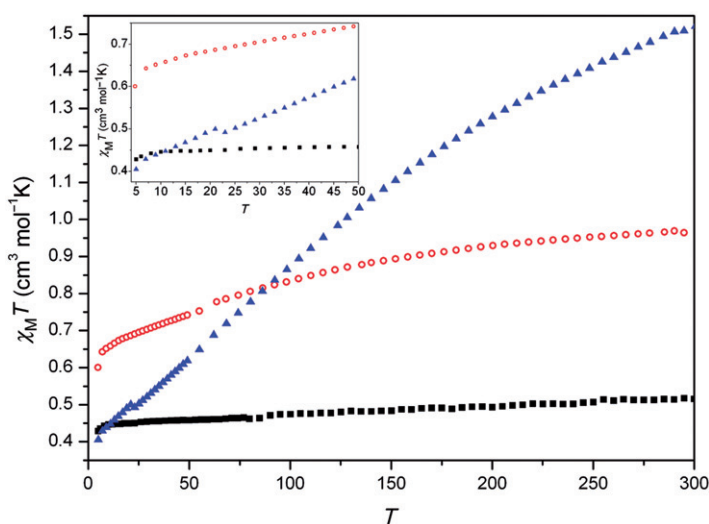


Figure 3. Plots of $\chi_M T$ vs. T for **1** (■), **2** (○), and **3** (▲).

when it starts to decrease first slowly, then abruptly to 5 K. The experimental $\chi_M T$ value at room temperature is $0.52 \text{ cm}^3 \text{ mol}^{-1} \text{ K}$, then decreases to $0.43 \text{ cm}^3 \text{ mol}^{-1} \text{ K}$ at 5 K, still larger than ($0.37 \text{ cm}^3 \text{ mol}^{-1} \text{ K}$) calculated for independent spin of one Cu(II) ($S=1/2$). Comparing the values between the experiment and calculation from 5 to 300 K, the effective magnetic moment comes from spin ($S=1/2$) and orbital contributions of Cu(II) because of the diamagnetic La(III) and large separation between Cu(II) ions. The decrease in the magnetic moment below 10 K could be attributed to weak lattice interactions. The values of θ and C for **1** are obtained from the least-squares fit of the data sets, which appear to follow the Curie–Weiss law. The low negative value (-6.37 K) of θ indicates weak antiferromagnetic interaction between metal centers. The magnetic property of Cu(II) ions in **1** can be used in the interpretation of magnetic interactions, which might exist in the rest of the isostructural complexes **2–4**, when non-magnetic La(III) is replaced by magnetic RE(III).

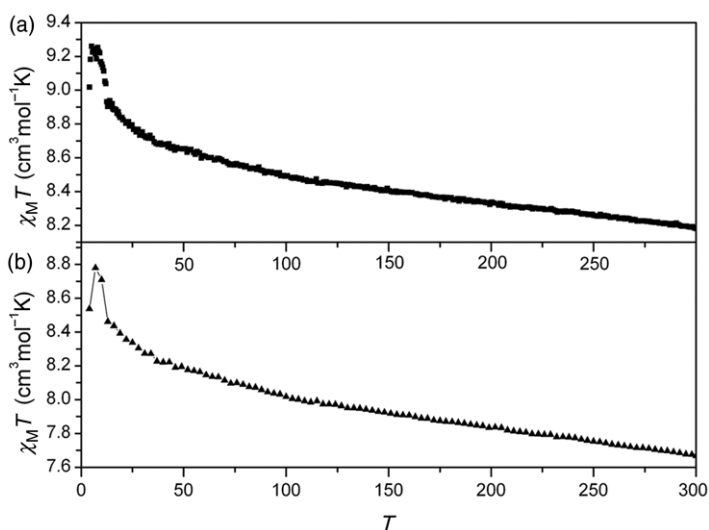


Figure 4. (a) Plots of $\chi_M T$ vs. T for $\{[\text{GdCuL}_4(\text{H}_2\text{O})_4]\text{L}_n\}$; (b) Plots of $\Delta\chi_M T$ ($\chi_M T_{(\text{Gd})} - \chi_M T_{(\text{Cu})}$) vs. T .

The $\chi_M T$ value of $0.96 \text{ cm}^3 \text{ mol}^{-1} \text{ K}$ at room temperature for **2** continuously decreases with temperature to $0.60 \text{ cm}^3 \text{ mol}^{-1} \text{ K}$ at 5 K. Different from **1**, the $\chi_M T$ values from 5 to 300 K are all less than that ($1.18 \text{ cm}^3 \text{ mol}^{-1} \text{ K}$) calculated for the sum of independent spin for Cu(II) ($S=1/2$) and spin-orbit coupling for Ce(III) ($S=1/2$). Since the cerium possesses an orbital contribution to the magnetic moment, the magnetic behavior of the Cu(II)–Ce(III) complex is more complicated than **1** and **4**. The observed $\chi_M T$ decrease may be due to two concomitant factors, depopulation of the Stark levels as T decreases and antiferromagnetic interaction between Cu(II) and Ce(III) [29–31].

From the plot of **3**, $\chi_M T$ of $1.52 \text{ cm}^3 \text{ mol}^{-1} \text{ K}$ at room temperature continuously diminishes with temperature to $0.41 \text{ cm}^3 \text{ mol}^{-1} \text{ K}$ at 5 K, which is very close to the Cu(II)-only value ($0.37 \text{ cm}^3 \text{ mol}^{-1} \text{ K}$). This may result from thermal depopulation of excited levels of Eu(III), leading to the copper(II)-only value in spite of the non-magnetic character of the ${}^7\text{F}_0$ ground state of Eu(III), and is obviously due to the van Vleck behavior of europium. The sharp decrease of $\chi_M T$ below 20 K may correspond to the combined effects of depopulation and intermolecular antiferromagnetism between the metallic ions. The magnetic behavior in **3** is similar to those in $\{[\text{Cu}_3\text{Ln}_2(\text{oda})_6(\text{H}_2\text{O})_6] \cdot 12\text{H}_2\text{O}\}_n$ [32] and $[(\text{acac})_2\text{Cr}(\text{ox})\text{Eu}(\text{HBPz}_3)_2]$ [33] complexes.

Because the ground state of Gd(III) is ${}^8\text{S}_{7/2}$ and the lowest excited state is very high, it is unnecessary to consider the contributions of the orbital angular momentum and the anisotropic effect when magnetism of the complex is discussed on the basis of electronic configuration. Compound **4** has a $\chi_M T$ value of $8.18 \text{ cm}^3 \text{ mol}^{-1} \text{ K}$ at room temperature (figure 4a), which nearly agrees with the expected value ($8.25 \text{ cm}^3 \text{ mol}^{-1} \text{ K}$) for the sum of independent spin for Cu(II) ($S=1/2$) plus Gd(III) ($S=7/2$). On lowering the temperature, $\chi_M T$ increases gradually before 11.7 K and rapidly rises to the maximum $9.26 \text{ cm}^3 \text{ mol}^{-1} \text{ K}$ at 5.2 K, and then decreases abruptly to $9.02 \text{ cm}^3 \text{ mol}^{-1} \text{ K}$ at 4.2 K.

Such increase of $\chi_M T$ values from 300 to 5.2 K indicates ferromagnetic interaction between Cu(II) and Gd(III) as the $\chi_M T$ values are much more than the spin-only value. At low temperature, $\chi_M T$ decreases with decreasing temperature, indicating intermolecular antiferromagnetic interactions. The magnetic properties of **4** are coincident with magnetic behaviors of [Gd(hfc)₃Cu(salen)] [34], Gd[Cu(PMOxd)]₄(ClO₄)₃ [35], and others [5–7].

Complex **4** has 1-D polycationic chains and its magnetic behavior like another Cu(II)–Gd(III) complex in which it was confirmed that the magnetic nature of 1-D chain has dinuclear character [36]. A quantitative analysis has been performed on the basis of an expression derived from the spin-only Hamiltonian $H = J_{\text{Cu-Gd}} S_{\text{Cu}} S_{\text{Gd}}$, where J is the exchange coupling parameter, and S_{Cu} and S_{Gd} are spin operators associated to the interacting spin centers. The theoretical expression for $\chi_M T$ is

$$\chi_M T = \frac{4N\beta^2 T}{k(T - \theta)} \frac{15g_4^2 + 7g_3^2 \exp(-\frac{4J}{kT})}{9 + 7 \exp(-\frac{4J}{kT})}$$

where g_4 ($g_4 = (7g_{\text{Gd}} + g_{\text{Cu}})/8$) and g_3 ($g_3 = (9g_{\text{Gd}} - g_{\text{Cu}})/8$) are the Zeeman factors associated with $S = 4$ and $S = 3$ low-lying states, respectively. Least-squares fitting of the experimental data led to the following set of parameters: $g_{\text{Gd}} = 2.00$, $g_{\text{Cu}} = 2.07$, $J = 2.62 \text{ cm}^{-1}$, $\theta = -0.45$ for **4**. The agreement factor R [$R = \Sigma(\chi_M T_{\text{Calcd}} - \chi_M T_{\text{Obs}})^2 / \Sigma(\chi_M T_{\text{Obs}})^2$] is 1.2×10^{-5} . The positive J indicates ferromagnetic coupling between Cu(II) and Gd(III). The magnetic properties of **4** also validate that the 1-D chain complex behaves as single dinuclear units.

The exchange coupling parameter J in **4** is not large, demonstrating that the coupling interaction between Cu and Gd is weak in a carboxylate-bridged system [25, 37–39].

As we have discussed above, the magnetic nature of **1** only comes from Cu(II) and the magnetic nature of **4** results from Cu(II), Gd(III), and Cu(II)–Gd(III) exchange interaction. $\Delta\chi_M T$ ($\chi_M T_{(\text{complex } 4)} - \chi_M T_{(\text{complex } 1)}$) can also be used to understand the Cu(II)–Gd(III) exchange interaction as the complexes are isostructural. Figure 4(b) shows that the $\Delta\chi_M T$ increases with the temperature and the Cu(II)–Gd(III) coupling is ferromagnetic.

4. Conclusion

Four heteronuclear isostructural RE–Cu (RE = La, Ce, Eu, and Gd) 2-D complexes consisting of [RECu(C₄H₅O₂)₄(H₂O)₄]⁺ cations and (C₄H₅O₂)[−] anions are synthesized. The eight-coordinate Gd(III) ions and four-coordinate Cu(II) are linked by carboxylate groups with alternating Cu(II)–RE(III) fragments to form chains along the *c*-axis in a nearly perfect line. The chains are joined through hydrogen bonding by anions to form a 2-D network along the *bc* planes. The number of coordinated carboxylates has important effect on the distance between Gd(III) and Cu(II). The four complexes display completely different magnetic phenomena between Cu(II) and RE. Complexes **1** and **2** are antiferromagnetic interactions, **4** exhibits ferromagnetic interaction, and Eu ions have van Vleck behavior in **3**.

Supplementary material

CCDC Nos. 693592, 195757, 196835, and 693845 for **1**, **2**, **3**, and **4** contain the supplementary crystallographic data for this article. These data can be obtained free of charge from The Cambridge Crystallographic Data Centre via www.ccdc.cam.ac.uk/data_request/cif

Acknowledgments

The authors would like to thank the Key Laboratory of Zhejiang University for collecting X-ray data and the Education Committee of Zhejiang Province, China, for providing funds.

References

- [1] G. Novitchi, S. Shova, A. Caneschi, J.P. Costes, M. Gdaniec, N. Stanica. *Dalton Trans.*, 1194 (2004).
- [2] G. Calvez, K. Bernot, O. Guillou, C. Daiguebonne, A. Caneschi, N. Mahé. *Inorg. Chim. Acta.*, **361**, 3997 (2008).
- [3] H.H. Zhao, N. Lopez, A. Prosvirin, H.T. Chifotides, K.R. Dunbar. *Dalton Trans.*, 878 (2007).
- [4] M. Ryazanov, V. Nikiforov, F. Lloret, M. Julve, N. Kuzmina, A. Gleizes. *Inorg. Chem.*, **41**, 1816 (2002).
- [5] I. Ramade, O. Kahn, Y. Jeannin, F. Robert. *Inorg. Chem.*, **36**, 931 (1997).
- [6] J.P. Costes, F.O. Dahan, G. Novitchi, V. Arion, S. Shova, J. Lipkowski. *Eur. J. Inorg. Chem.*, 1530 (2004).
- [7] M.L. Kahn, C. Mathoniere, O. Kahn. *Inorg. Chem.*, **38**, 3692 (1999).
- [8] H.Z. Kou, Y.B. Jiang, A.L. Cui. *Cryst. Growth Des.*, **5**, 77 (2005).
- [9] J.P. Costes, F. Dahan, A. Dupuis. *Inorg. Chem.*, **39**, 5994 (2000).
- [10] J.P. Costes, F. Dahan, A. Dupuis, J.P. Laurent. *Inorg. Chem.*, **39**, 169 (2000).
- [11] C. Benelli, A.J. Blake, P.E.Y. Milne, J.M. Rawson, R.E.P. Winpenny. *Chem. Eur. J.*, **1**, 614 (1995).
- [12] J.L. Sanz, R. Ruiz, A. Gleizes, F. Loret, J. Faus, M. Julve, J.J. Borrás-Almenar, Y. Journaux. *Inorg. Chem.*, **35**, 7384 (1996).
- [13] F. He, M.L. Tong, X.M. Chen. *Inorg. Chem.*, **44**, 8285 (2005).
- [14] B. Wu, W.M. Lu, X.M. Zheng. *J. Coord. Chem.*, **56**, 65 (2003).
- [15] W.M. Lu, B. Wu, X.M. Zheng. *J. Chem. Cryst.*, **30**, 777 (2000).
- [16] B. Wu, W.M. Lu, X.M. Zheng. *J. Chem. Cryst.*, **33**, 203 (2003).
- [17] B. Wu, W.M. Lu, X.M. Zheng. *Transition Met. Chem.*, **28**, 323 (2003).
- [18] Y. Zhu, W.M. Lu, F. Chen. *Acta Cryst.*, **60**, 1459 (2004).
- [19] Y. Zhu, W.M. Lu, M. Ma, F. Chen. *Acta Cryst.*, **E61**, 1610 (2005).
- [20] F. Chen, W.M. Lu, Y. Zhu, B. Wu, X.M. Zheng. *J. Coord. Chem.*, **62**, 808 (2009).
- [21] W.M. Lu, Z.P. Shao, J.B. Hu, X.Y. Lao, J.M. Gu. *J. Coord. Chem.*, **40**, 145 (1996).
- [22] J.L. Yi, Z.Y. Fu, S.J. Liao. *J. Coord. Chem.*, **62**, 2290 (2009).
- [23] G.M. Sheldrick. *SHELXTL 6.10*. Bruker AXS, Madison, WI, USA (2000).
- [24] D.T. Cromer, J.T. Waber. *International Tables for X-ray Crystallography*, Kynoch Press, Birmingham (1974).
- [25] X.M. Chen, Y.L. Wu, Y.Y. Yang, S.M.J. Aubin, D.N. Hendrickson. *Inorg. Chem.*, **37**, 6186 (1998).
- [26] F. He, M.L. Tong, X.L. Yu, X.M. Chen. *Inorg. Chem.*, **44**, 559 (2005).
- [27] R. Baggio, M.T. Garland, Y. Moreno, O. Peña, M. Pereg, E. Spodine. *J. Chem. Soc., Dalton Trans.*, 2061 (2000).
- [28] H.Y. Wu, N. Wang, S.T. Yue, Y.L. Liu. *J. Coord. Chem.*, **62**, 2511 (2009).
- [29] M.L. Kahn, T.M. Rajendiran, Y. Jeannin, C. Mathoniere, O. Kahn. *C.R. Acad. Sci. Paris, Serie IIC Chimie*, **3**, 131 (2000).
- [30] C. Benelli, A.J. Blake, P.E.Y. Milne, J.M. Rawson, R.E.P. Winpenny. *Chem. Eur. J.*, **1**, 614 (1995).
- [31] M.L. Kahn, C. Mathoniere, O. Kahn. *Inorg. Chem.*, **38**, 3692 (1999).
- [32] R. Baggio, M.T. Garland, Y. Moreno, O. Peña, M. Pereg, E. Spodine. *J. Chem. Soc., Dalton Trans.*, 2061 (2000).

- [33] T. Sanada, T. Suzuki, T. Yoshida, S. Kaizaki. *Inorg. Chem.*, **37**, 4712 (1998).
- [34] R.L. Carlin. *Magnetochemistry*, Springer-Verlag, Berlin (1986).
- [35] N. Zhou, B. Liu, Y. Ma, D. Wang, D.Z. Liao. *J. Coord. Chem.*, **62**, 1134 (2009).
- [36] G. Novitchi, J.P. Costes, B. Donnadieu. *Eur. J. Inorg. Chem.*, 1808 (2004).
- [37] X.M. Chen, Y.L. Wu, Y.X. Tong, Z. Sun, D.N. Hendrickson. *Polyhedron*, **16**, 4265 (1997).
- [38] A. Panagiotopoulos, T.F. Zafirooulos, S.P. Perlps, E. Balkalbasis, I. Masson-Ramada, O. Kahn, A. Terzis, C.P. Raptopoulou. *Inorg. Chem.*, **34**, 4918 (1995).
- [39] K. Manseki, Y. Kitakami, M. Sakamoto, H. Sakiyama, A. Matsumoto, Y. Sadaoka, Y. Nishida, M. Sakai, Y. Fukuda, M. Ohba, H. Okawa. *J. Coord. Chem.*, **48**, 1 (1999).